Nanoscale Research Letters
a SpringerOpen Journal

NANO EXPRESS Open Access

Electrochemical performance of $Ni_xCo_{1-x}MoO_4$ ($0 \le x \le 1$) nanowire anodes for lithium-ion batteries

Kyung-Soo Park, Seung-Deok Seo, Hyun-Woo Shim and Dong-Wan Kim*

Abstract

$Ni_xCo_{1-x}MoO_4$ ($0 \le x \le 1$) nanowire electrodes for lithium-ion rechargeable batteries have been synthesized via a hydrothermal method, followed by thermal post-annealing at 500°C for 2 h. The chemical composition of the nanowires was varied, and their morphological features and crystalline structures were characterized using field-emission scanning electron microscopy and X-ray powder diffraction. The reversible capacity of $NiMoO_4$ and $Ni_{0.75}Co_{0.25}MoO_4$ nanowire electrodes was larger (≈520 mA h/g after 20 cycles at a rate of 196 mA/g) than that of the other nanowires. This enhanced electrochemical performance of $Ni_xCo_{1-x}MoO_4$ nanowires with high Ni content was ascribed to their larger surface area and efficient electron transport path facilitated by their one-dimensional nanostructure.

Introduction

Among the types of anode materials available for rechargeable lithium-ion batteries, graphite has been commercialized. However, because of its drawbacks, such as capacity limitations (theoretical capacity of 372 mA h/g), initial loss of capacity, and structural deformation [1,2], one of the current areas of interest in lithium-ion battery research is the search for new anode candidates that have large reversible capacities. In the past decade, transition metal oxides (M_xO_y, M = Co, Ni, Cu, Fe) that can deliver a high reversible capacity by conversion reaction mechanisms ($M_xO_y + ne^- + nLi^+ \leftrightarrow xM^0 + Li_nO_y$) have been considered as an alternative to commercial graphite anodes for lithium-ion batteries [3-10].

Metal molybdates, $AMoO_4$-type compounds (where A is a divalent metal ion), have attracted the interest of researchers because of their electronic and magnetic properties and their many applications, such as catalysis and photoluminescence [11-14]. Recently, $CoMoO_4$ and $NiMoO_4$, synthesized with nanowire morphology by a simple hydrothermal method, were exploited as materials for lithium-ion batteries but were only applied as cathodes [15,16].

In this paper, we report the fabrication of $Ni_xCo_{1-x}MoO_4$ ($0 \le x \le 1$) nanowire electrodes by a hydrothermal method, followed by thermal post-annealing. We also demonstrate the superior electrochemical performance of $Ni_xCo_{1-x}MoO_4$ nanowires for lithium-ion battery anodes.

Experimental details

$Ni_xCo_{1-x}MoO_4$ ($0 \le x \le 1$) nanowires were synthesized by a simple hydrothermal method, in which high purity Ni $(NO_3)_2{\cdot}6H_2O$ (99.999%; Sigma-Aldrich, Saint Louis, MO, USA), $Co(NO_3)_2{\cdot}6H_2O$ (98%; Sigma-Aldrich, Saint Louis, MO, USA), and $Na_2MoO_4{\cdot}2H_2O$ (99.5%; Sigma-Aldrich, Saint Louis, MO, USA) were used as source materials, followed by post-annealing at an elevated temperature. Initially, to prepare a clean solution (total cationic concentration of 0.1 M) with a molar fraction (x) of Ni (x = 0, 0.25, 0.5, 0.75, and 1), controlled amounts of Co- and Ni-containing reagents were dissolved in deionized water (80 mL) under constant magnetic stirring; then, the solution was added to an aqueous solution (80 mL) containing 0.1 M of $Na_2MoO_4{\cdot}2H_2O$. This resulting solution was transferred into a Teflon-lined stainless steel autoclave, sealed, and maintained at 180°C for 8 h. After the reaction was completed, the resulting solid products were harvested by centrifugation, washed with deionized water and acetone several times, and then dried at 60°C for 6 h in a vacuum oven. Finally, the as-prepared hydrate

* Correspondence: dwkim@ajou.ac.kr
Department of Materials Science and Engineering, Ajou University, Suwon, 443-749, Republic of Korea

Springer

© 2012 Park et al; licensee Springer. This is an Open Access article distributed under the terms of the Creative Commons Attribution License (http://creativecommons.org/licenses/by/2.0), which permits unrestricted use, distribution, and reproduction in any medium, provided the original work is properly cited.

nanowire precursors were post-annealed at 500°C for 2 h to dehydrate them.

The morphologies and crystal structures of the prepared $Ni_xCo_{1-x}MoO_4 \cdot nH_2O$ and $Ni_xCo_{1-x}MoO_4$ ($0 \le x \le 1$) nanowires were investigated using field-emission scanning electron microscopy [FE-SEM] (10 kV; FEI NOVA, Tokyo, Japan) and X-ray powder diffraction [XRD] (λ_{CuKa} = 1.5405 Å; Miniflex II, Rigaku, Tokyo, Japan). The thermal behavior of the as-prepared hydrate samples was analyzed by thermogravimetric analysis [TGA] (DTG-60H, Shimadzu, Kyoto, Japan). For TGA, the samples were heated from room temperature up to 800°C at a heating rate of 10°C/min in air.

For the electrochemical evaluation of the $Ni_xCo_{1-x}MoO_4$ ($0 \le x \le 1$) nanowires, positive electrode films were cast on a Cu foil by mixing each nanowire powder (1 to 2 mg) with Super P carbon black (MMM Carbon, Brussels, Belgium) and Kynar 2801 binder (PVdF-HFP, Arkema Inc., King of Prussia, PA, USA) in a mass ratio of 70:15:15. The assembled Swagelok-type cells composed of a positive electrode, negative electrode (lithium metal-foil), and separator film (Celgard 2400, Celgard LLC, Charlotte, NC, USA) saturated with a liquid electrolyte consisting of $LiPF_6$ (1 M) dissolved in a solution of ethylene carbonate and dimethyl carbonate (1:1 *v*/*v*) were cycled at voltages between 0.01 and 3.0 V using an automatic battery cycler (WBCS 3000, WonaTech, Seoul, South Korea).

Results and discussion

Figures 1a to 1e show typical FE-SEM images of as-prepared $Ni_xCo_{1-x}MoO_4 \cdot nH_2O$ precursors with various cationic compositions. All of the samples were of nanowire morphology regardless of their compositional differences. However, the diameters and lengths of the nanowires tended to decrease with increasing Ni concentration. As shown in Figure 1e, the $NiMoO_4 \cdot nH_2O$ nanowires were agglomerated acutely and even formed clusters that were several microns in size. The agglomeration of the nanowires might be due to strong attractive forces between the small-sized nanowire particles. The crystalline structures of the as-prepared $Ni_xCo_{1-x}MoO_4 \cdot nH_2O$ nanowires were confirmed from their XRD patterns, as seen in Figure 1f. The XRD patterns taken from all $Ni_xCo_{1-x}MoO_4 \cdot nH_2O$ nanowires agreed well with previously reported patterns for $CoMoO_4 \cdot nH_2O$ (JCPDS no.: 26-0477).

The dehydration process was investigated using the thermogravimetric [TG] technique; the results of which are shown in Figure 2. The typical TG curves obtained from the $Ni_xCo_{1-x}MoO_4 \cdot nH_2O$ nanowires in the temperature range from 30°C to 800°C showed net weight losses of 7% to 9% for each sample. This weight loss was mainly attributed to the evolution of species related to water molecules, such as reversibly bound water molecules (low temperature), water molecules forming an integral part of the crystal structure of $Ni_xCo_{1-x}MoO_4 \cdot nH_2O$ (medium temperature), and water molecules reversibly bound to the hydrate crystal phase (high temperature) [14,15]. On the basis of the TG results, the post-annealing temperature for all the hydrate samples was 500°C, at which almost all water molecules were removed sufficiently to form $Ni_xCo_{1-x}MoO_4$ nanowires.

Figures 3a to 3e show FE-SEM images of $Ni_xCo_{1-x}MoO_4$ ($0 \le x \le 1$) nanowires obtained by post-annealing the $Ni_xCo_{1-x}MoO_4 \cdot nH_2O$ nanowire precursors at 500°C for 2 h. All post-annealed samples maintained their pristine nanowire morphologies. Although a marked change in the diameter or length of the nanowires after post-annealing was not observed, they seemed to be agglomerated slightly and were forming bundles, which could lead to a decrease in their surface area. In order to confirm the change in surface area that may have occurred during post-annealing of $Ni_xCo_{1-x}MoO_4 \cdot nH_2O$ nanowire precursors, the Brunauer-Emmett-Teller [BET] (Belsorp-mini, BEL Japan Inc., Osaka, Japan) technique was carried out at liquid nitrogen temperature. From the results presented in Table 1 it can be confirmed that the surface areas of $Ni_xCo_{1-x}MoO_4$ nanowires in all compositions were slightly decreased compared with those of the corresponding $Ni_xCo_{1-x}MoO_4 \cdot nH_2O$ nanowires. This was ascribed to the aggregation and growth of the nanowires. Furthermore, it was found that the surface areas of the nanowires gradually increased with increasing Ni concentration because of the corresponding decrease in their diameter and length.

To investigate the crystal structures of the $Ni_xCo_{1-x}MoO_4$ nanowires, their XRD patterns were examined carefully. The XRD patterns obtained for the $CoMoO_4$ and $NiMoO_4$ nanowires in Figure 3f corresponded well with their bulk materials (JCPDS nos.: 25-1434, 21-0868, 33-0948, and 45-0142 for α-$CoMoO_4$, β-$CoMoO_4$, α-$NiMoO_4$, and β-$NiMoO_4$, respectively). However, as can be seen in Figure 3f, both end-members had α- and β-phases corresponding to each material together. It is known that single-phase β-$CoMoO_4$ and α-$NiMoO_4$ can be formed by fast cooling and by slow cooling, respectively, to room temperature after post-annealing of their hydrates [14,17,18]. Meanwhile, D. Vie et al. reported that the α-$CoMoO_4$ phase became detectable as a minority phase after heat treatment of the amorphous solid precursor at a temperature above 700°C [17]. On the basis of these reports, we believe that the coexistence of α- and β-phases in $CoMoO_4$ and $NiMoO_4$ nanowires can be attributed to the medium cooling rate (≈10°C/min to 30°C/min) applied after post-annealing or to a change of phase transition temperature with the unique morphologies of the samples.

Among the $Ni_xCo_{1-x}MoO_4$ nanowires with a medium composition, the XRD pattern of the $Ni_{0.25}Co_{0.75}MoO_4$ nanowires agreed well with that of $CoMoO_4$. However, in contrast with that observed for pure $CoMoO_4$, the

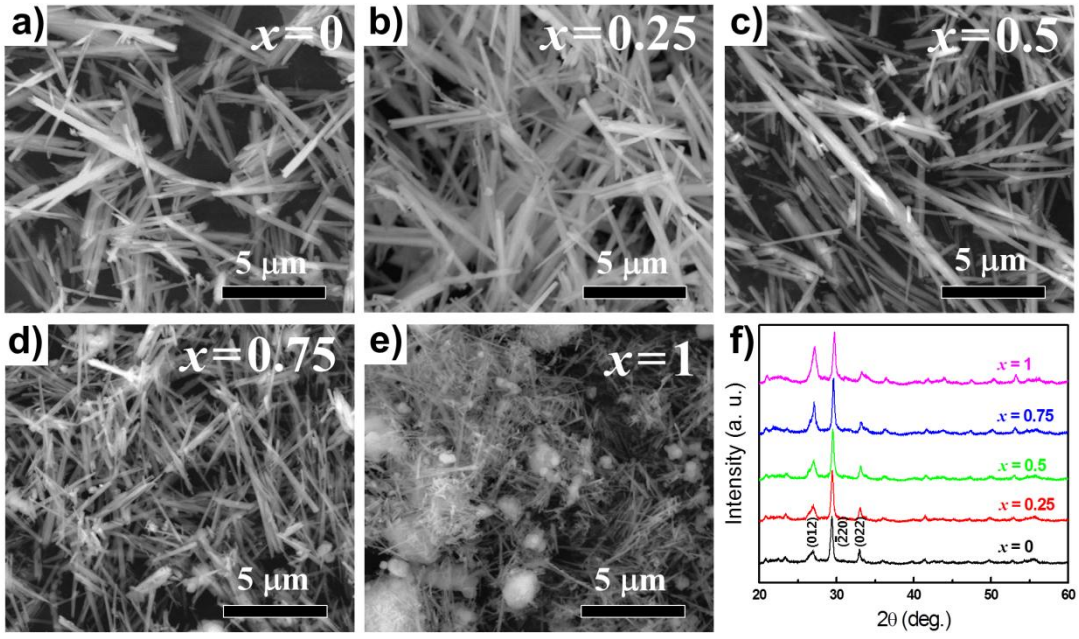

Figure 1 Morphologies and crystal structures of $Ni_xCo_{1-x}MoO_4{\cdot}nH_2O$ nanowires. (**a-e**) Typical FE-SEM images of as-prepared $Ni_xCo_{1-x}MoO_4{\cdot}nH_2O$ nanowire precursors with various *x* values and (**f**) their corresponding X-ray diffraction patterns (by KS Park et al.).

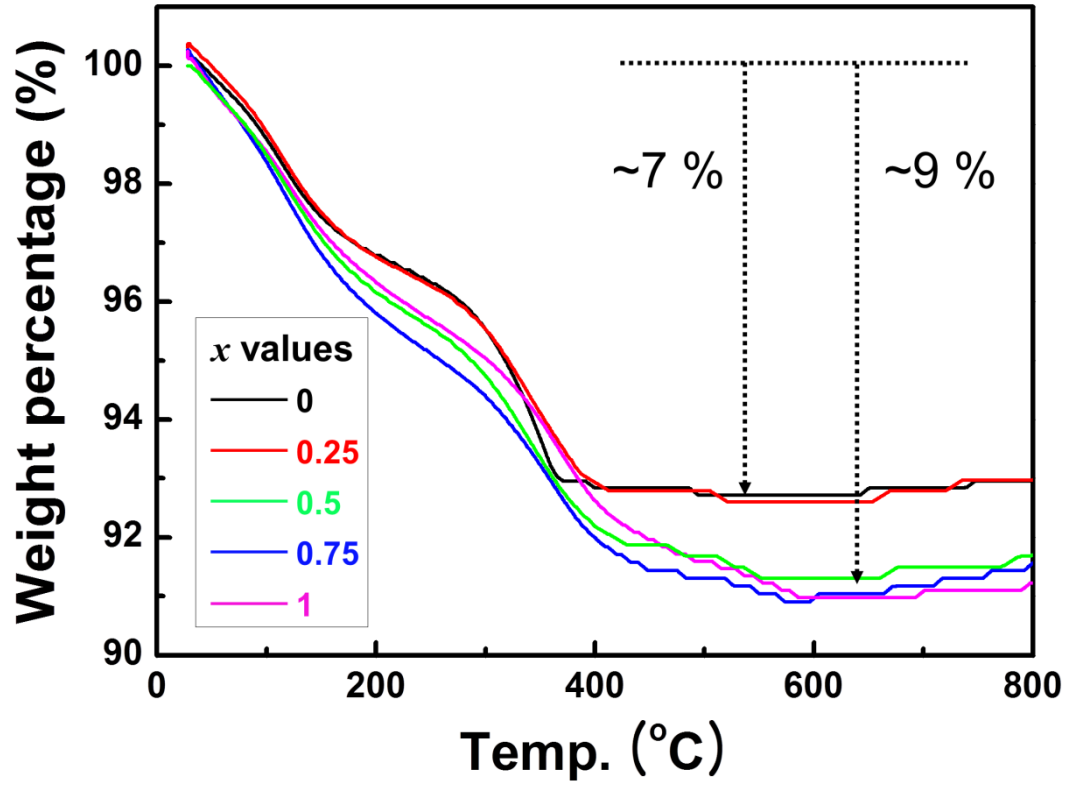

Figure 2 Thermal behavior of $Ni_xCo_{1-x}MoO_4{\cdot}nH_2O$ nanowires. TG curves for as-prepared $Ni_xCo_{1-x}MoO_4{\cdot}nH_2O$ nanowire precursors with various values of *x*, heating at a rate of 10°C/min in air (by KS Park et al.).

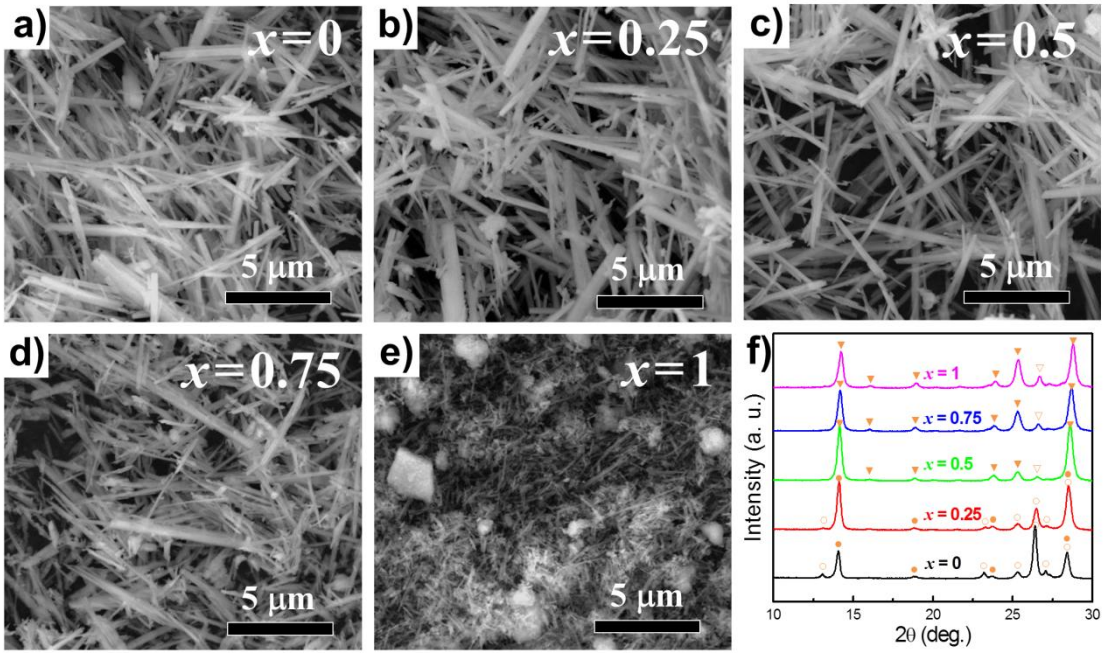

Figure 3 Morphologies and crystal structures of $Ni_xCo_{1-x}MoO_4$ nanowires. (**a-e**) FE-SEM images of $Ni_xCo_{1-x}MoO_4$ nanowires with various *x* values and (**f**) their corresponding X-ray diffraction patterns. Filled circle, empty circle, filled inverted triangle, and empty inverted triangle correspond to α-$CoMoO_4$, β-$CoMoO_4$, α-$NiMoO_4$, and β-$NiMoO_4$, respectively (by KS Park et al.).

peaks corresponding to α-$CoMoO_4$ became more dominant compared with those of β-$CoMoO_4$, indicating that relative intensities of the diffraction peaks of the α-phase increase with Ni content [17]. In the case of the $Ni_{0.5}Co_{0.5}MoO_4$ nanowires, it was found that the XRD pattern corresponded closer with pure $NiMoO_4$ than with pure $CoMoO_4$ (Figure 3f). This implies that the basic crystal structure of the nanowires was transformed from $CoMoO_4$-related structures into $NiMoO_4$-related structures. The XRD pattern of the $Ni_{0.75}Co_{0.25}MoO_4$ nanowires also agreed with that of pure $NiMoO_4$. It should be noted that no secondary phases, such as NiO and CoO, were detected in any of the XRD patterns, which indicated that $CoMoO_4$ and $NiMoO_4$ formed solid solutions perfectly.

Table 1 Surface areas of prepared samples

	$Ni_xCo_{1-x}MoO_4 \cdot nH_2O$	$Ni_xCo_{1-x}MoO_4$
x value	Surface area (m^2/g)	
0	9.5	7.8
0.25	10.1	9.0
0.5	12.7	10.3
0.75	21.0	18.6
1	47.4	39.2

Comparison of surface areas for as-prepared $Ni_xCo_{1-x}MoO_4 \cdot nH_2O$ and $Ni_xCo_{1-x}MoO_4$ nanowires dehydrated at 500°C for 2 h (by KS Park et al.).

In general, most reports on the lithium reactivity of molybdates have been focused on their application as anode materials for lithium-ion batteries because they could deliver high reversible capacity through a conversion reaction with lithium [19-21]. Moreover, NiO and CoO have also been known as anode materials, reacting with lithium by an equivalent mechanism with a molybdate [3]. On the basis of such knowledge, we expected the following electrochemical reaction mechanism of $Ni_xCo_{1-x}MoO_4$ with lithium:

$$Ni_xCo_{1-x}MoO_4 + 8Li^+ + 8e^- \rightarrow xNi + (1-x)Co + Mo + 4Li_2O \quad (1)$$

$$xNi + (1-x)Co + Mo + 4Li_2O \leftrightarrow xNiO + (1-x)CoO + MoO_3 + 8Li^+ + 8e^- \quad (2)$$

To evaluate the electrochemical performance of the $Ni_xCo_{1-x}MoO_4$ nanowire electrodes, typical voltage-specific capacity curves were recorded at a current rate of C/5 (≈196 mA/g; note that 1 C ≈ 980 mA/g on the basis of the reaction in Equation 2) in a potential window between 0.01 and 3.0 V (Figure 4). In the first discharge reaction, samples containing nickel reacted with lithium at a lower potential region (≈0.4 V to 0.01 V) compared with the $CoMoO_4$ nanowire electrode (≈0.3 V to 0.01 V). Notably, the first discharge capacities for $Ni_{0.75}Co_{0.25}MoO_4$ and $NiMoO_4$ were higher than their theoretical capacities; this might be ascribed to the formation of the solid electrolyte interface-like organic layer. Subsequent

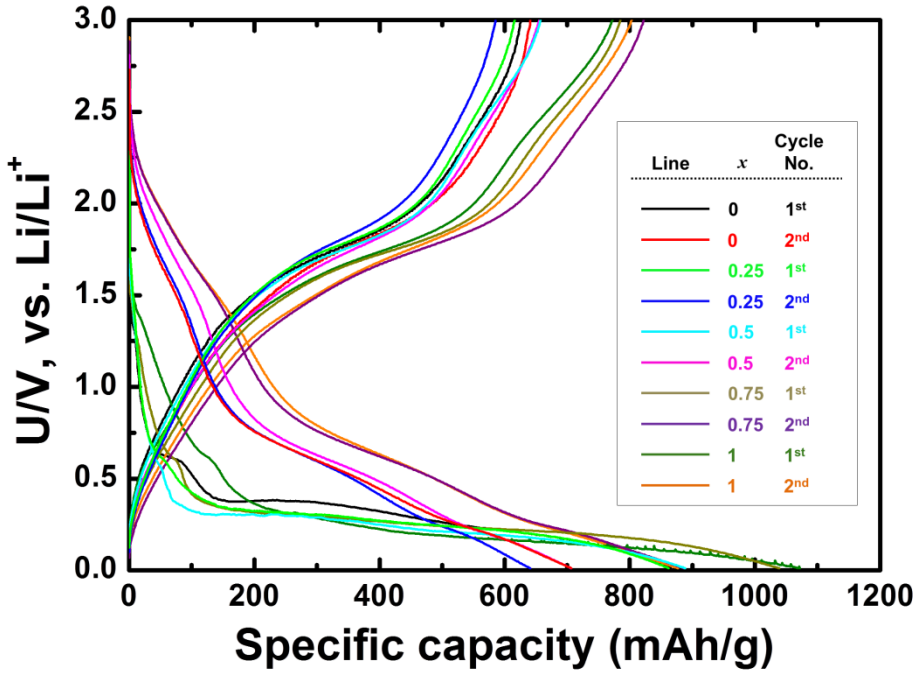

Figure 4 Charging-discharging curves of $Ni_xCo_{1-x}MoO_4$ nanowire electrodes. Charging-discharging curves of the $Ni_xCo_{1-x}MoO_4$ nanowire electrodes with various *x* values at a rate of C/5 (by KS Park et al.).

second discharge-charge reactions occurred reversibly on the basis of the reaction in Equation 2. These highly reversible capacities of $Ni_xCo_{1-x}MoO_4$ nanowire electrodes could be an evidence for delivering capacity by conversion mechanism.

Figure 5 shows the specific capacity of $Ni_xCo_{1-x}MoO_4$ nanowire electrodes versus the cycle number at a current rate of C/5. When the values of *x* were 0, 0.25, and 0.5, the reversible capacities of $Ni_xCo_{1-x}MoO_4$ nanowire electrodes faded rapidly even during the initial cycles, resulting in a poor reversible capacity of ≈290 mA h/g after 20 cycles. This result was attributed to the small surface areas of the nanowire electrodes. From the BET results summarized in Table 1 it was found that their surface areas were very small compared with those of the other nanowires, which led to a small electrode/electrolyte interface, resulting in a poor reversible capacity. Meanwhile, the reversible capacity of the $Ni_xCo_{1-x}MoO_4$ nanowire electrodes with *x* values of 0.75 and 1 (≈520 mA h/g after 20 cycles) was larger than that of the previously mentioned three nanowire electrodes because of the increased electrode/electrolyte interface that resulted from the larger surface area of the nanowires (Table 1). In accordance with the BET results, the electrochemical performance of the $NiMoO_4$ nanowire electrode was expected to be vastly superior compared with that of the $Ni_{0.75}Co_{0.25}MoO_4$ nanowire electrode. However, the electrochemical performances of both electrodes were similar, as shown in Figure 5 due to the aggregation of the $NiMoO_4$ nanowires. When we fabricated the positive electrode, the carbon black that is commonly used as a conducting additive was mechanically mixed with the nanowires as the active material. At that time, clusters formed by aggregation of the $NiMoO_4$ nanowires could not be mixed efficiently with carbon black, which resulted in impairing their electrochemical performance by restriction of the electronic conduction paths from each nanowire to a current collector. In contrast, the $Ni_{0.75}Co_{0.25}MoO_4$ nanowires did not form such clusters during the synthesis process. For this reason, the $Ni_{0.75}Co_{0.25}MoO_4$ nanowire electrode could deliver a reversible capacity as high as the $NiMoO_4$ nanowire electrode. Furthermore, the $Ni_{0.75}Co_{0.25}MoO_4$ nanowire electrode exhibited a superior coulombic efficiency of ≈95% (Figure 5).

Conclusion

In summary, we have successfully synthesized $Ni_xCo_{1-x}MoO_4$ ($0 \le x \le 1$) nanowire electrodes by employing a hydrothermal method to prepare hydrate nanowires, followed by post-annealing of the as-prepared hydrate nanowires. Although α- and β-phases coexisted in all of the nanowire samples, no secondary phases were detected, indicating that $CoMoO_4$ and $NiMoO_4$ formed perfect solid solutions. Compared with the reversible capacity (≈290 mA h/g after 20 cycles) of the $Ni_xCo_{1-x}MoO_4$

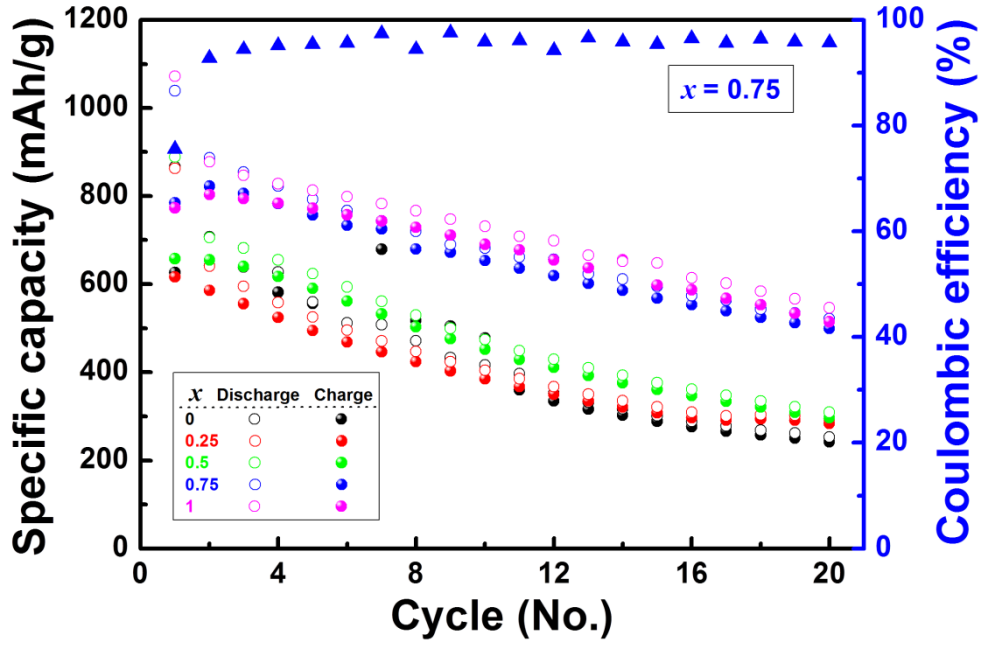

Figure 5 Electrochemical properties of $Ni_xCo_{1-x}MoO_4$ nanowire electrodes. Variation of the discharge (open circles)-charge (solid circles) specific capacity and coulombic efficiency (solid triangle) versus the cycle number at a rate of C/5 for the $Ni_xCo_{1-x}MoO_4$ nanowire electrodes with various *x* values (by KS Park et al.).

nanowire electrodes with *x* values of 0, 0.25, and 0.5, the reversible capacity of the nanowire electrodes containing a higher Ni content (*x* = 0.75 and 1) increased more (≈520 mA h/g after 20 cycles). Despite the difference in surface area between the $NiMoO_4$ and $Ni_{0.75}Co_{0.25}MoO_4$ nanowires, the reason for the observation of their similar reversible capacities was because of the agglomeration of $NiMoO_4$ nanowires and the resulting restriction of the electronic conduction paths from each nanowire to a current collector. We anticipate that this approach will facilitate the tailoring of other electrodes based on solid solution materials, to provide electrodes with superior electrochemical performance.

Acknowledgements
This work was supported by the National Research Foundation of Korea (NRF) grant funded by the Korea government (MEST; nos. 2010-0029617 and 2011-0005776).

Authors' contributions
K-SP carried out the $Ni_xCo_{1-x}MoO_4$ ($0 \le x \le 1$) nanowire sample preparation and drafted the manuscript. S-DS and H-WS participated in microstructural and electrochemical analyses. D-WK designed the study, led the discussion of the results, and participated in writing the manuscript. All authors read and approved the final manuscript.

Competing interests
The authors declare that they have no competing interests.

Received: 2 September 2011 Accepted: 5 January 2012
Published: 5 January 2012

References

1. Disma F, Aymard L, Dupont L, Tarascon JM: **Effect of mechanical grinding on the lithium intercalation process in graphites and soft carbons.** *J Electrochem Soc* 1996, **143**:3959.
2. Disma F, Lenain C, Beaudoin B, Aymard L, Tarascon JM: **Unique effect of mechanical milling on the lithium intercalation properties of different carbons.** *Solid State Ionics* 1997, **98**:145.
3. Poizot P, Laruelle S, Grugeon S, Dupont L, Tarascon JM: **Nano-sized transition-metal oxides as negative-electrode materials for lithium-ion batteries.** *Nature* 2000, **407**:496.
4. Taberna PL, Mitra S, Poizot P, Simon P, Tarascon JM: **High rate capabilities Fe_3O_4-based Cu nano-architectured electrodes for lithium-ion battery applications.** *Nat Mater* 2006, **5**:567.
5. Kim DW, Ko YD, Park JG, Kim BK: **Formation of lithium-driven active/inactive nanocomposite electrodes based on $Ca_3Co_4O_9$ nanoplates.** *Angew Chem Int Ed* 2007, **46**:6654.
6. Shim HW, Jin YH, Seo SD, Lee SH, Kim DW: **Highly reversible lithium storage in *Bacillus subtilis*-directed porous Co_3O_4 nanostructures.** *ACS Nano* 2011, **5**:443.
7. Li Y, Tan B, Wu Y: **Mesoporous Co_3O_4 nanowire arrays for lithium ion batteries with high capacity and rate capability.** *Nano Lett* 2008, **8**:265.
8. Shim HW, Cho IS, Hong KS, Cho WI, Kim DW: **Li electroactivity of iron (II) tungstate nanorods.** *Nanotechnology* 2010, **21**:465602.
9. Lee GH, Park JG, Sung YM, Chung KY, Cho WI, Kim DW: **Enhanced cycling performance of Fe^0/Fe_3O_4 nanocomposite electrode for lithium-ion batteries.** *Nanotechnology* 2009, **20**:295205.
10. Ko YD, Kang JG, Choi KJ, Park JG, Ahn JP, Chung KY, Nam KW, Yoon WS, Kim DW: **High rate capabilities induced by multi-phasic nanodomains in iron-substituted calcium cobaltite electrodes.** *J Mater Chem* 2009, **19**:1829.
11. Liu J, Huang X, Li Y, Li Z: **A general route to thickness-tunable multilayered sheets of sheelite-type metal molybdate and their self-assembled films.** *J Mater Chem* 2007, **17**:2754.
12. Vilminot S, André G, Kurmoo M: **Magnetic properties and magnetic structure of $Cu^{II}_3Mo^{VI}_2O_9$.** *Inorg Chem* 2009, **48**:2687.
13. Chu WG, Wang HF, Guo YJ, Zhang LN, Han ZH, Li QQ, Fan SS: **Catalyst-free growth of quasi-aligned nanorods of single cryatal $Cu_3Mo_2O_9$ and their catalytic properties.** *Inorg Chem* 2009, **48**:1243.

14. Rodriguez JA, Chaturvedi S, Hanson JC, Albornoz A, Brito JL: **Electronic properties and phase transformations in $CoMoO_4$ and $NiMoO_4$: XANES and time-resolved synchrotron XRD studies.** *J Phys Chem B* 1998, **102**:1347.
15. Xiao W, Chen JS, Li CM, Xu R, Lou XW: **Synthesis, characterization, and lithium storage capability of $AMoO_4$ (A = Ni, Co) nanorods.** *Chem Mater* 2010, **22**:746.
16. Ding Y, Wan Y, Min YL, Zhang W, Yu SH: **General synthesis and phase control of metal molybdate hydrates $MMoO_4$•nH_2O (M = Co, Ni, Mn, n = 0, 3/4, 1) nano/microcrystals by a hydrothermal approach: magnetic, photocatalytic, and electrochemical properties.** *Inorg Chem* 2008, **47**:7813.
17. Vie D, Martínez E, Sapiña F, Folgado JV, Beltrán A: **Freeze-dried precursor-based synthesis of nanostructured cobalt-nickel molybdates $Co_{1-x}Ni_xMoO_4$.** *Chem Mater* 2004, **16**:1697.
18. Rodriguez JA, Chaturvedi S, Hanson JC, Brito JL: **Reaction of H_2 and H_2S with $CoMoO_4$ and $NiMoO_4$: TPR, XANES, time-resolved XRD, and molecular-orbital studies.** *J Phys Chem B* 1999, **103**:770.
19. Kim SS, Ogura S, Ikuta H, Uchimoto Y, Wakihara M: **Reaction mechanisms of $MnMoO_4$ for high capacity anode material of Li secondary battery.** *Solid State Ionics* 2002, **146**:249.
20. Leroux F, Goward GR, Power WP, Nazar LF: **Understanding the nature of low-potential Li uptake into high volumetric capacity molybdenum oxides.** *Electrochem Solid-State Lett* 1998, **1**:255.
21. Sharma N, Shaju KM, Rao GVS, Chowdari BVR, Dong ZL, White TJ: **Carbon-coated nanophase $CaMoO_4$ as anode material for Li ion batteries.** *Chem Mater* 2004, **16**:504.

doi:10.1186/1556-276X-7-35
Cite this article as: Park *et al.*: Electrochemical performance of $Ni_xCo_{1-x}MoO_4$ ($0 \le x \le 1$) nanowire anodes for lithium-ion batteries. *Nanoscale Research Letters* 2012 **7**:35.

Submit your manuscript to a SpringerOpen journal and benefit from:

► Convenient online submission
► Rigorous peer review
► Immediate publication on acceptance
► Open access: articles freely available online
► High visibility within the field
► Retaining the copyright to your article

Submit your next manuscript at ► springeropen.com